Continental-scale trends of daily precipitation records in late 20th century decades and 21st century projections: An analysis of observations, reanalyses and CORDEX-CORE projections

Lara Belleri[1], James M. Ciarlo[2], Maurizio Maugeri[3], Roberto Ranzi[1], Filippo Giorgi[2]

[1]*Università degli Studi di Brescia, Department of Civil, Environmental Architectural Engineering, and Mathematics, Brescia, Italy*
[2]*Abdus Salam International Centre for Theoretical Physics (ICTP), Trieste, Italy*
[3]*Università degli Studi di Milano, Department of Environmental Science and Policy, Milano, Italy*

Corresponding author: Filippo Giorgi, Abdus Salam ICTP, Trieste. email: giorgi@ictp.it

Keywords: extreme events, precipitation, precipitation change, precipitation records

Abstract

We apply a methodology to identify and count records (events of unprecedented intensity) in daily precipitation time series to two sets of data: 1) different observational and reanalysis products for recent decades; and 2) 21st century projections (RCP8.5 and RCP2.6 scenarios) completed with two regional climate models driven by three global climate models over nine continental-scale domains. Comparison of the detected (or actual) number of records with the corresponding number theoretically expected in stationary climate conditions (or "reference" number of records) provides indications of trends in daily precipitation extremes, as expected in a changing climate. In particular, we measure deviations from stationary conditions using the ratio of actual to reference records (RAtR) as a basic metric. We find that the observational products provide mixed indications of precipitation record trends across regions, while in the reanalysis products and the model simulations for the historical period the RAtR value shows a prevailing increasing trend with time over most continents. The RAtR shows a consistent and pronounced increase in all RCP8.5 continental-scale projections, when sustained warming occurs throughout the 21st century, while smaller to no significant trends are found in the RCP2.6 scenario, when the warming stabilizes after about mid-21st century. These results are indicative of an increase in precipitation extremes with global warming as measured by the higher number of local precipitation events of unprecedented intensity compared to what expected in stationary climate conditions, although a marked variability of this response is found across different regions. Our method can have useful applications in detection and attribution of hydroclimatic extremes and in impact and vulnerability assessment studies.

1. Introduction

One of the most robust responses of the climate system to global warming is an increase in the intensity of precipitation events and extremes associated with the greater energy and water vapor content of the atmosphere, the latter being related to the Clausius-Clapeyron equation (e.g., Trenberth et al. 2003, Giorgi et al. 2011, 2014a, 2019; Held and Soden 2016;

Martinkova and Kysely 2020). Analysis of global and regional climate model projections has indeed indicated a pervasive future increase in extreme precipitation events for different climate warming scenarios, as for example measured by metrics such as the 95th or 99th percentiles of the daily precipitation distribution, although there is spatial variability in this response and not all regions will experience equally strong increases in extreme precipitation (e.g., Sillmann et al. 2013; Giorgi et al. 2014b, 2019; Coppola et al. 2021). Increased occurrence of events of unprecedented intensity has also been reported in analyses of model projections (e.g., Giorgi et al. 2019), which has profound implications for implied impacts and vulnerabilities of natural and socio-economic systems.

In a previous paper, Giorgi and Ciarlo (2022) (hereafter referred to as GC22) adapted a technique for identifying and counting the number of record breaking events (or more simply "records", i.e., events of unprecedented intensity) to daily precipitation time series as a tool to assess the response of precipitation extremes to global warming. This technique is a variant of an analogous method used for investigating trends in daily temperature records as an indication of global warming (e.g., Elguindi et al. 2013; Meehl et al. 2016; Jones 2016; Powell and Delage 2019). Specifically, the variant introduced by GC22 was designed to account for the occurrence of large numbers of 0 values (dry days) in daily precipitation time series, differently from temperature time series (see section 2).

GC22 applied this technique to different observation and reanalysis products for the European region, along with regional climate model (RCM) projections carried out under the EURO-CORDEX framework (Jacob et al. 2020). They found a prevailing increase in the number of precipitation records compared to those theoretically expected under stationary climate conditions. This finding was especially evident when aggregating results over the European region, and was found both in observations for the last several decades and future climate projections under different scenarios. The study of GC22 also revealed how trends in precipitation records exhibit substantial spatial variability and can depend on the climatic regime of a region. Therefore, in order to assess the robustness and potential use of the record methodology, it is important to investigate whether the behavior of precipitation records across different areas of the globe shows consistent features.

Based on these considerations, in the present paper we extend the study of GC22 to different continental-scale regions covering most land areas of the world. After having analysed four centennial datasets of daily precipitation observed at Italian rain gauges, we analyse regional gridded observation datasets over seven regions for the historical period 1950-2020 and then compare results with three reanalysis products. Then we turn our attention to the recently completed CORDEX-CORE ensembles of RCM projections for nine continental scale domains under forcing from two greenhouse gas (GHG) concentration pathways (see Giorgi et al. 2022 and references therein). Our primary aim here is to investigate to what extent the conclusions of GC22 are extendable to different regional contexts both in observations from the past and projections for the future. We stress that our study is mostly of diagnostic nature, as a process-based investigation of specific regional responses of precipitation records to projected changes in global climate would entail targeted analyses that are well beyond the purpose of a single paper.

In the next section we first describe the basic features of the methodology devised by GC22 to identify and count daily precipitation records, along with the datasets employed in our study. The results are then discussed in section 3 and our main conclusions are reported in section 4.

2. Methods and data.

2.1 The GC22 record identification method

The identification of a record in a daily time series of a given variable, for example temperature (e.g. Elguindi et al. 2013), occurs when, at a certain point and for a given day of the year (e.g., June 15) and a given year, the daily value of the variable is greater than all corresponding values on the same day of the year in all previous years of the time series. Under stationary climate conditions, the expected rate of records for any year k, $E_{rr}(k)$, is a function of time after the starting year which follows a theoretical power law given by (Arnold et al., 1998; Elguindi et al., 2013)

$$E_{\mathrm{rr}}(k) = 1/k \qquad (1)$$

where k is the year beginning from the start of the time series. The number of records for the year k (E_k), which we refer to as "reference" number of records, is then expressed as $1/k$ multiplied by the number of days in the year (or season/month, depending on the focus of the analysis). In other words, in the first year $k = 1$, and each day of the year is considered a record, leading to $E_1 = 365$; in the second year $k = 2$, and records are expected to occur in half of the days of the year, therefore $E_2 = E_1/2 = 182.5$, and so on, following a power law decrease of the number of reference records. If the actual number of records in a time series is significantly different from this theoretical estimate, there is a deviation from stationarity, indicating the presence of trends in the selected time series. Note that the validity of Eq. (1) depends on the assumption of no autocorrelation in the time series, and since we are comparing here daily precipitation in different years this assumption can be considered as appropriate.

The direct application of this methodology to precipitation is however problematic, since a specific feature of daily precipitation is that it is characterized by a large and in fact dominant number of dry days, i.e., days with 0 precipitation (e.g., Trenberth et al. 2007). The validity of Eq. (1) can thus be called into question because of the excessively small sample size of significant daily precipitation amounts in a series of k years. To circumvent this problem, GC22 proposed to use as variable the maximum daily precipitation in a consecutive 30-day period, which effectively removes most 0 values in the series, since in most locations it is very likely that at least one rainy day is found in a 30-day period. In fact, any length of consecutive days can be used in this approach. Therefore, for a given day of the k^{th} year, the value of E_k is not calculated using the precipitation of that day of the year (e.g., June 15) but the maximum daily precipitation in a 30-day period centered around that day (e.g., June 1-30).

Specifically, in order to calculate the number of daily precipitation records in a year, we use the following procedure. For a given point, we first look for the maximum precipitation value in each 30 day running period of the year centered around a given day, and therefore we start the calculation on January 15 and end it on December 17, i.e. we cover 337 30-day running periods of the year. For each 30 day running period we then calculate the maximum daily precipitation and compare it with the analogous values from all previous years, and if it is the highest one, then we have a record. We then normalize the number of records thus obtained over the entire year by the total number of running 30-day periods in the year, i.e. 337. In this way, we obtain a frequency of records per year. Note that this normalization renders the results comparable not only with the theoretical estimate of Eq. (1) but also across different approaches, for example using different lengths of running periods or using non overlapping 12 months in the year (in this latter case, for example, the normalization factor would be 12).

One caveat of this approach pointed out by GC22 is that the occurrence of particularly intense precipitation events in different points may affect records for strings of days, although this effect is minimized by the normalization described above. In addition, in relatively dry regions and/or seasons, even over a 30-day period there is still a significant occurrence of dry events. Finally, for an individual local time series there can be a substantial number of years without records, along with years with several records, and this yields a large temporal variability of detected records. This is for example shown by the time series of the frequency of the centennial daily precipitation records found at four locations in northern Italy presented in Figure 1, where the interannual variability in the number of records and the substantial number of years with 0 records is evident (see Marani and Zanetti 2015, Maugeri et al. 2002, Scolozzi and Eccel 2017 for the series description).

For all these reasons, the GC22 methodology is best applied at the regionally aggregated level. Specifically, for a given grid, after using the procedure described above to calculate at each grid point of a region the number of actual records for each year, we simply sum the number of records across all grid points of the selected region and normalize this sum by the total number of grid points in the region. This value of regionally aggregated actual records can then be compared with the reference value of Eq. (1) by using as metric the ratio of actual-to-reference number of records (hereafter referred to as RAtR). Note that in the framework of the GC22 paper, we tested this methodology against using 12 separate month long periods or choosing a 15 day running period (instead of 30) and found that the results where qualitatively consistent across the different methods, thereby concluding that our approach is robust. It should be pointed out, however, that the rolling window approach is helpful to obtain smoother time series and RAtRs, but the values it produces are not directly representative of annual daily record count.

2.2 Observation, reanalysis and climate model data

Here we apply the GC22 daily precipitation record identification procedure to the following datasets: i) four regional gridded observation products, i.e. E-OBS (Cornes et al. 2018; here we use the version V23 at 0.1 degree resolution) for Europe, IMD (Pai et al. 2014) for the Indian sub-continent, NAmerEXT (Livneh et al. 2015) covering both the

North and Central America regions, APHRODITE (Yatagai et al. 2012), covering the East Asia, Southeast Asia and Middle East regions; ii) three reanalysis products (ERA5, Hersbach et al. 2020; MERRA-2 (Gelaro et al. 2017, hereafter referred to as MERRA); JRA-55 (Kobayashi et al. 2015, hereafter referred to as JRA); and iii) the CORDEX-CORE experiments, including for nine continental domains an ensemble of 12 projections with two RCMs (the ICTP RegCM4, Giorgi et al. 2012; and the GERICS REMO, Jacob et al. 2012), for two GHG concentration pathways, (the high end RCP8.5 and low end RCP2.6 Moss et al. 2010) and three driving Global Climate Models (GCMs) used in the Climate Model Intercomparison Project 5 (CMIP5, Taylor et al. 2012): HadGEM (Jones et al. 2011); MPI (Giorgetta et al. 2013); and NorESM (Bentsen et al. 2013), i.e. a high, mid and low climate sensitivity model, respectively. Note that for a few domains these GCMs were replaced by other ones due to their poor performance over the selected region (see Giorgi et al. 2022), and specifically the RegCM runs employed GFDL-ESN2M (Dunne et al. 2012) over the Central America domain instead of NorESM, and MIROC5 (Watanabe et al. 2010) over the South Asia domain instead of HadGEM. The RCM grid spacing for these simulations is ~25 km except for the European region, where it is ~ 12 km. For more information on the CORDEX-CORE ensembles the reader is referred to Giorgi et al. (2022) and references therein.

All the observation, reanalysis and projection datasets employed in our analysis are listed in Table 1. Note that there are global daily precipitation datasets also available, but they either are defined at coarse spatial resolutions or cover relatively short observation periods, and therefore they are not used here. Also, we highlight that the E-OBS dataset is continuously updated and while GC22 used the version V20 at 0.25 degree resolution, here we use the more recent version V23 at 0.1 degree resolution. The two versions actually differ significantly in some regions, and these differences affect the full area average, which may lead to different results compared to GC22. More information on these EOBS updates can be found at https://www.ecad.eu/download/ensembles/download.php#datafiles.

We divide our analysis in two parts. In the first, we compare observations and reanalysis data over the seven observation sub-domains colored in red in Figure 2, with the purpose to i) assess the presence of trends of RAtR in the observations over the different regions; and ii) assess whether the different reanalysis products reproduce these trends and provide a consistent signal. In the second part of the paper, we move to the model projections over the nine CORDEX-CORE domains of Figure 2: Europe (EUR), Africa (AFR), South Asia (SAS), East Asia (EAS), Southeast Asia (SEA), Australasia (AUS), North America (NAM), Central America (CAM), and South America (SAM). In this case we employ a larger number of domains than in the observation analysis for two reasons: i) it is not the purpose of this paper to compare model simulations and observations over specific regions, since the model experiments were not set up specifically for the purpose of reproducing regional patterns; ii) the observation sub-domains do not include important regions such as Africa, South America and Australia, which are instead present in the CORDEX-CORE ensemble. Nevertheless, the model analysis regions do not include the full CORDEX-CORE domains but sub-regions that attempt to match the corresponding observation domains as much as possible (see Figure 2). The main aim of the analysis of the CORDEX-

CORE projections is to assess the behavior of daily precipitation records in a climate warming context, and to identify whether there are qualitative similarities with the observed trends.

Note that for the observation sub-domains we use the same name as the model domain which encompasses it, even though they do not have the same extent. The only observation sub-domain which is not fully included in a CORDEX domain is the Middle East (ME) one.

3. Results

3.1 Analysis of observations and reanalyses for the historical period

Figures 3a and 3b show two sets of panels for each observation sub-domain, each observation dataset and the three reanalysis products: the left panels report the original yearly values of the frequency of occurrence of actual records, along with the theoretical reference curve from Eq. (1); the right panels show the 10-year running average of the yearly RAtR values and the corresponding linear trend fit line, along with its linear regression coefficient and p-value calculated using the NCL package, which employs an ANOVA-based approach, as described on the website https://www.ncl.ucar.edu/Document/Functions/Contributed/regline_stats.shtml.

The observations (black curves in Figs. 3a and 3b), exhibit a marked variability in the behavior of records across the different regions. In some regions, most noticeably EAS, the number of detected records follows the reference curve quite closely in both the observations and reanalysis datasets, with RAtR values close to 1 and small and not statistically significant trends. These cases are indicative of a near stationary behavior of precipitation extremes, and they show that our approach of using 30-day running windows is indeed capable of capturing such stationary conditions. In other cases, namely EUR, SAS, and ME, the actual and reference values diverge in the observations after 1-2 decades from the beginning of the time series, with RAtR being mostly greater than 1 and showing positive linear trends, although statistically significant at the 95% confidence level only in EUR. This indicates an increase in precipitation records compared to the reference value, and it is thus suggestive of an increase in maximum precipitation intensity during recent decades. Finally, for the SEA, NAM and CAM regions, the RAtR is predominantly greater than 1, but with negative trend lines. Therefore, the observation datasets do not indicate a consistent behavior of precipitation records across regions, although a prevalence of RAtR values greater than 1 is seen. This regional variability may also be associated with the possibly large uncertainties underlying station-based precipitation products due to the sparsity and heterogeneity of station locations along with measurement problems, e.g., the gauge undercatch (Adam & Lettenmaier, 2003).

We can put our observation results in a broader context by a qualitative comparison with Fig. SPM-3 of IPCC (2021), which reports regions where significant changes in heavy precipitation (defined as the 95th or 99th percentile of 1-day or 5-day precipitation, depending on the study) during recent decades have been observed. IPCC reports significant increases of heavy precipitation over most of Europe, the Middle East and India regions, with non significant changes over most of Central and North America, results that are qualitatively in line with our record analysis. On the other hand, while we do not find significant trends in RAtR values over East and Southeast Asia, IPCC reports significant increases in heavy precipitation.

Moving to the reanalyses, we can first see from the right panels of Figure 3 that in the majority of cases (with some notable exceptions such as NAM) there is a general agreement in the RAtR interdecadal variations between the observation and reanalysis data, as for example is particularly evident in the European region. This points to the fact that, at least for these regional cases, the reanalyses offer a reasonably good representation of the observed variability of extremes. Despite this agreement, however, the trends are in some instances quite different between observations and reanalyses, or across reanalysis products, not only in magnitude but also in sign.

As a matter of fact, although in the reanalyses there is a more pronounced prevalence of positive trends than in the observations, both the observations and the reanalysis products do not indicate a fully consistent signal in terms of RAtR trends across regions. It is difficult to attribute these different behaviors to specific factors, however we can hypothesize that a significant factor is that the reanalysis precipitation data are still a product of models utilizing different physics parameterizations and data assimilation procedures, and these may evidently have an effect on the simulation of precipitation extremes, thereby representing an important element of uncertainty.

3.2 Analysis of the model projections

We now turn our attention to the model projections analyzed over the nine domains shown in Figure 2. As an illustrative example, Figure 4 shows for the RCP8.5 scenario and all nine continental scale domains of Figure 2 (land only) the 10-yr running average and trend fit lines for the RAtR in the RegCM4, REMO and driving MPI CORDEX-CORE projections, i.e., the projections driven by the intermediate sensitivity GCM. The data are reported from 1970 to 2099 and are separated in two segments for which different trend lines are calculated: 1970-2020, to represent the historical period; and 2020-2099, to represent the future period. For the historical period, trends are calculated for the GCM and RCM projections as well as the three reanalysis products, where we stress that for these calculations the domains and analysis periods are different from those used in Figure 3 and thus in some instances different trends are found even for the same reanalysis product.

The most ubiquitous and consistent signal in Figure 4 is a strong and highly statistically significant increase in RAtR in both the GCM and RCM projections for the future period, with RAtR values greater than 1 and mostly statistically significant positive trends. This is a clear indication of a pronounced deviation from stationary climate conditions induced by the sustained 21st century warming in the RCP8.5 scenario, resulting in a much greater number of daily precipitation records (up to factors exceeding 2) compared to the stationary reference conditions.

Some exceptions to this behavior, however, do occur. The main one is the Australia region, where we find pronounced interdecadal variations in the RAtR values with low statistical significance of trends in the MPI and REMO runs. A possible reason for this behavior is that most of the Australia region is covered by desert and semi-desert regions, with large numbers of dry days, so that even some relatively small numbers of precipitation occurrences can affect the regional average number of records, thereby enhancing the interdecadal variability. Other cases of low statistical significance of trends are the CAM (REMO and RegCM runs) and AFR (MPI and REMO runs) regions, which also include large desert and semi-desert areas.

Although a predominant increasing RAtR signal is found in the projections, Figure 4 also shows that the trend can be different across the GCM and RCM simulations. In particular, over several regions the RAtR trends are greater in the driving MPI model than in the corresponding nested RCM simulations, and are mostly greater in the RegCM4 than the REMO simulations, even though these RCMs are driven by the same GCMs. It is difficult to identify unambiguously the reasons for this behavior, which however illustrates the sensitivity of simulated extreme precipitation to the different model configurations and physics parameterizations.

Figure S1 shows the same statistics as Figure 4, but for the RCP2.6 scenario, for which the warming essentially stabilizes, or is even slightly reduced, after the mid-decades of the 21st century (Teichmann et al. 2021). In this case we find that, although in most cases the RAtR values are still greater than 1, the trends calculated over the 21st century are either negligible (and statistically not significant) or negative. Again, this result is consistent with the fact that the warming in the RCP2.6 scenario is mostly stable throughout the late portion of the 21st century, with no significant changes in precipitation extremes.

The RAtR trends for the historical period show more mixed results, also affected by the pronounced interdecadal variability of the RAtR signal over some regions. We find a mix of cases with trends of different sign, magnitude and statistical significance, not only across regions, but also across models and reanalysis products. We should note that precipitation extremes are characterized by pronounced temporal and spatial variability, and this clearly influences the relatively wide spread of results. Reducing this uncertainty through methods, such as ours, aimed at extracting and quantifying relevant information on extremes is important for developing adaptation policies.

In order to obtain a clearer overall picture of the RAtR trends in the historical period, Figure 5a reports the RAtR regional trend values in all GCM, RCM and reanalysis products for the period 1970-2020, while Figure 5b shows the corresponding multi-model averages of RCM, GCM and reanalysis trends (note that for MERRA the trends are calculated over a shorter time period). The latter should filter out some of the natural variability of the individual time series. Clearly, there is a large predominance of positive trends, although a number of these trend values are small and with low statistical significance. In six out of nine regions there is either full agreement in the sign of the trend across models and reanalyses (NAM, EUR, EAS) or only one outlier (SAM, SAS, SEA). Over SAM and EUR the trends are more significant in the reanalysis than the models, while the opposite is found over EAS, SEA and NAM. As also found in Section 3.1, the regions for which the signal is more mixed are AUS, AFR, and CAM, which encompass large desert areas.

The multi-model average trends (Figure 5b) show good agreement in sign, and for some cases magnitude, across models and reanalyses over all regions except AUS and AFR, where one case of negative value is found. Therefore, Figure 5b shows that an increase of the frequency of daily precipitation records compared to the reference value is a prevailing signal also for the historical period across most regions in the model simulations and reanalysis products.

Figures 6 and 7 finally summarize the future period (2020-2099) linear trend values of the RAtR for the RCP8.5 and RCP2.6 scenarios, respectively, in all RegCM4 and REMO projections. We find that in the RCP8.5 scenario, (Fig. 6) for all regions and model combinations, except the GFDL-driven RegCM4 CAM run, the trends are positive, with largest values over the North America, East Asia and Southeast Asia regions, and lowest values in Central America. In the vast majority of cases the positive trends are statistically significant at the 95% confidence level. We also find that the Australian region is the only one in which the NorESM driven projections, i.e., those employing the GCM with lowest climate sensitivity, present larger positive trends than the other ones.

By comparison, the RCP2.6 scenario (Figure 7) produces small RAtR trends, mostly not statistically significant, and fairly equally distributed between positive and negative values. The most noticeable cases are the East Asia and Southeast Asia regions, where the trends are predominantly negative and statistically significant. We recall that in the RCP2.6 scenario global warming stabilizes or even tends to decrease after the mid-21st century, and therefore the presence of negative RAtR trends is not inconsistent with the corresponding global warming trend. In fact, stabilization of global temperatures would imply a decrease in records in line with Eq. 1 and a reduction of temperatures would lead to record values even lower than those obtained from Eq. 1.

As already mentioned, the increase of heavy precipitation in climate projections, in particular for the high end GHG concentration pathways, is a consolidated result (e.g. Sillmann et al. 2014; Giorgi et al. 2014;2019; IPCC 2021) and is generally in line with our findings. Both the models and the reanalysis products also indicate a prevalence of positive and increasing RAtR values during the historical period, which is also in line with the assessment of IPCC (2021), as is a less clear signal over regions such as Australia, Africa and central America. Therefore, we conclude that our record-based analysis is at least qualitatively consistent with the results from the use of more traditional extreme precipitation analyses.

4. Summary and Conclusions

In this paper we have used the methodology recently described by GC22 to identify and count records (i.e., events of local unprecedented intensity) in time series of daily precipitation events. This is a variant of the standard record detection method used for temperature and is designed to account for the occurrence of large numbers of zero values (i.e., dry days) in the time series. The method uses as indicator the maximum precipitation amount in a rolling window of 30-days and therefore it should be recognised that the values it produces are not directly representative of annual daily record counts, as for example in the analogous approach for daily temperature records.

We applied the technique to different station-based observation datasets and reanalysis products for recent decades, along with 21st century RCM projections under the RCP8.5 and RCP2.6 scenarios completed as part of the CORDEX-CORE project (Giorgi et al. 2022). The analysis is carried out for two sets of domains. The CORDEX-CORE data, along with corresponding reanalysis data for the historical period, are analyzed over nine continental scale regions (land only areas) encompassed within the corresponding CORDEX-CORE domains. The analysis of observations and corresponding reanalyses is instead carried out over a smaller set of sub-domains where high resolution observations are actually available.

The basic scientific question we address here is whether the increase in intensity of precipitation expected under global warming conditions (e.g., Sillmann et al.2013, Giorgi et al. 2019) is reflected into a widespread increase in the occurrence of daily precipitation records with respect to those expected from stationary climate conditions (Eq. 1), and how this response varies across regions.

The station-based observation datasets for the last decades provide mixed results, in the sense that the RAtR exhibits both positive and negative trends over different regions, although a prevalence of RAtR values treater than 1 is found. Corresponding record counts from the reanalysis products show interdecadal variations mostly in line with observations, however the actual trends are sometimes different between observations and reanalyses or across reanalysis products. The extension of the analyses to all CORDEX domains for the common period 1970-2020 shows prevailing positive trends during the historical period 1970-2020, but still with significant variability across regions, reanalysis and model products. In particular, Australia, central America and Africa emerge as the regions characterized by the most pronounced interdecadal variability of the RAtR values, resulting in more mixed trend results. This could at least to some extent be due to the presence of large desert areas with small numbers of precipitation events which can affect the regional averages. In addition, the pronounced natural variability of regional precipitation, and especially extremes, likely contributes to the pronounced spread found in the historical period.

Coming to the projections, in the high-end RCP8.5 scenario a consistent and mostly statistically significant signal of positive RAtR trend is found in all regions, except for one projection over Central America. The RAtR trends are small, of both signs, and mostly not statistically significant in the RCP2.6 scenario, where the warming does not increase in the second half of the century, implying stabilised conditions of precipitation extremes.

Overall, our more extensive and globally based analysis supports the findings of GC22 in that the use of our modified precipitation record identification method can be an effective tool to detect the occurrence of precipitation events of unprecedented local intensity (i.e. precipitation records) associated with global warming. This conclusion is especially evident when sustained warming occurs, such as in the RCP8.5 scenario. In cases of more moderate warming, such as during recent decades, the results from observation data, reanalyses and model simulations are less conclusive, although with a prevalence of positive RAtR trends. In addition, the results are characterized by substantial variability across regional climatic regimes, and in particular the method may need to be refined for application to semi-arid regions characterized by small numbers of precipitation events and pronounced interannual variability.

As daily precipitation observation time series increase in length and quality of coverage, we thus assess that the GC22 approach can give an important contribution to detection and attributions studies of hydroclimatic extremes, an area of increasing interest within the global warming debate. The method can clearly also have useful applications in the assessment of the impact of extremes, especially when the emphasis is on extremes of unprecedented intensity.

Acknowledgements

We acknowledge the E-OBS dataset from the EU-FP6 project UERRA (http://www.uerra.eu) and the Copernicus Climate Change Service, and the data providers in the ECA&D project (https://www.ecad.eu).
-The APHRODITE datasets can be found at the APHRODITE website (http://aphrodite.st.hirosaki-u.ac.jp)
-The IMD dataset is available thanks to the Indian Meteorological Department (https://dsp.imdpune.gov.in/)
-The NAmerEXT dataset is available thanks to the Lawrence Livermore National Laboratory (ftp://192.12.137.7/pub/dcp/archive/OBS/livneh2014.1_16deg/)
-ERA5 is produced on the ECMWF high-performance computing facility and is available on the CDS cloud server (**https://cds.climate.copernicus.eu/**)
-MERRA is produced by NASA Global Modeling and Assimilation Office (GMAO) and available on Goddard Earth Sciences Data and Information Services Center website (https://disc.gsfc.nasa.gov/datasets/M2T1NXFLX_5.12.4/summary)
-JRA-55 has been produced with the TL319 version of the Japan Meteorological Agency (JMA) operational data assimilation system (https://rda.ucar.edu/datasets/ds628.0/)
-The CORDEX-CORE data can be found at the Earth System Grid Federation data-nodes (https://esgf.llnl.gov/).
We would like to also thank Marco Marani of Università degli Studi di Padova and Andrea Cicogna of the Regional Meteorological Observatory (OSMER) of ARPA Friuli-Venezia Giulia, for providing the historical daily precipitation series of Padova and Trieste, respectively. The Po River Water District funded the project “Caratterizzazione del regime di frequenza degli estremi idrologici nel distretto Po, anche considerando scenari di cambiamento climatico ”, which supported the first and fourth authors. Finally, we would

like to thank two anonymous reviewers for their extremely careful and constructive reviews, which helped to improve the quality of the paper.

Data Source:

The scripts used for the method of this paper (developed from the GC22 paper) are freely available on Github (https://github.com/ciarloj/Climate-Records-processor)

References:

Adam JC, Lettenmaier DP (2003) Adjustment of global gridded precipitation for systematic bias. J Geophys Res 108(D9):4257, doi:10.1029/2002JD002499

Arnold BC, Balakrishnan N, Nagaraja HN (1998) Records. John Wiley, New York, doi:10.1002/9781118150412

Bentsen M, Bethke I, Debernard J.B, et al. (2013) The Norwegian Earth System Model, NorESM1-M – Part 1: Description and basic evaluation of the physical climate. Geosci. Model Dev, 6:687–720, doi:10.5194/gmd-6-687-2013.

Coppola E, Raffaele F, Giorgi F, et al. (2021) Climate hazard indices projections based on CORDEX-CORE, CMIP5 and CMIP6 ensembles. Clim Dyn, doi: 10.1007/s00382-021-05640-z.

Cornes R, van der Schrier G, van der Besselaar EJM, et al. (2018) En ensemble version of the E-OBS temperature and precipitation datasets. J Geophys Res Atmos 123, doi: 10.1029/2017JD028200.

Dunne J.P, et al. (2012) GFDL’s ESM2 Global Coupled Climate-Carbon Earth System Models. Part I: Physical Formulation and Baseline Simulation Characteristics. Journal of Climate, 25:6646-6665, doi:10.1175/JCLI-D-11-00560.1.

Elguindi N, Rauscher SA, Giorgi F (2013) Historical and future changes in maximum and minimum temperature records. Clim Change 117:415-431, doi: 10.1007/s10584-012-0528-z

Gelaro R, et al. (2017) The Modern-Era Retrospective Analysis for Research and Applications, Version 2 (MERRA-2). J. Clim, 30(14):5419–5454, doi:10.1175/JCLI-D-16-0758.1.

Giorgetta MA, Jungclaus J, Reick CH, et al. (2013) Climate and carbon cycle changes fom 1850 to 2100 in mpi-esm simulations for the coupled model intercomparison project Phase 5. Journal of Advances in Modeling the Earth System 5:572-597, doi:10.1002/jame.20038

Giorgi F, Im E-S, Coppola E, et al. (2011) Higher hydroclimatic intensity with global warming. J Clim, 24:5309-5324, doi:10.1175/2011JCLI3979.1

Giorgi F, Coppola E, Solmon F, et al. (2012) RegCM4: Model description and preliminary tests over multiple CORDEX domains. Clim Res 52:7–29, doi:10.3354/cr01018

Giorgi F, Coppola E, Raffaele F, et al. (2014b) Changes in extremes and hydroclimatic regimes in the CREMA ensemble projections. Clim. Change 125:39-51, doi:10.1007/s10584-014-1117-0

Giorgi F, Coppola E, Raffaele F (2014a) A consistent picture of the hydroclimatic response to global warming from multiple indices: Models and observations. J Geophys Res 119:11,695-11,708, doi:10.1002/2014JD022238

Giorgi F, Raffaele F, Coppola E (2019) The response of precipitation characteristics to global warming from climate projections. Earth Sys Dyn 10: 73-89, doi:10.5194/esd-10-73-2019

Giorgi F, Coppola E, Jacob D, Teichmann C, Abba Omar S, et al. (2022) The CORDEX CORE EXP-I initiative: Description and highlight results from the initial analysis. Bull Am Met Soc, doi: 10.1175/BAMS-D-21-0119.1.

Giorgi F, & Ciarlo` JM (2022) Use of daily precipitation records to assess the response of extreme events to global warming: Methodology and illustrative application to the European region. Int J Climatol 1– 10, doi:10.1002/joc.7629

Held IM, Soden BJ (2016) Robust responses of the hydrological cycle to global warming. J Climate 19:5686-5699, doi:10.1175/JCLI3990.1

Hersbach H, Bell B, Berrisphord P (2020) The ERA5 global reanalysis. Quart J Roy Met Soc 146:1999-2049, doi:10.1002/qj.3803

IPCC, 2021: Climate Change 2021: The Physical Science Basis. Contribution of Working Group I to the Sixth Assessment Report of the Intergovernmental Panel on Climate Change [Masson-Delmotte V, Zhai P, Pirani A, Connors SL, Péan C, Berger S, Caud N, Chen Y, Goldfarb L, Gomis MI, Huang M, Leitzell K, Lonnoy E, Matthews JBR, Maycock TK, Waterfield T, Yelekçi O, Yu R, and Zhou B (eds.)]. Cambridge University Press, Cambridge, United Kingdom and New York, NY, USA, In press, doi:10.1017/9781009157896.

Jones C.D, Hughes J.K, Bellouin N, et al (2011) The HadGEM2-ES implementation of CMIP5 centennial simulations, Geosci. Model Dev, 4:543–570, doi:10.5194/gmd-4-543-2011.

Jones P (2016) The reliability of global and hemispheric temperature records. Adv Atmos Sci 33:269-282, doi:10.1007/s00376-015-5194-4

Jacob D, Elizalde A, Haensler A, et al. (2012) Assessing the transferability of the regional climate model REMO to different coordinated regional climate downscaling experiment (CORDEX) regions. Atmosphere 3:181–199, doi:10.3390/atmos3010181.

Jacob D, Teichmann C, Sobolowski S et al. (2020) Regional climate downscaling over Europe: perspectives from the EURO-CORDEX community. Reg Env Change 20, doi:10.1007/s10113-020-01606-9.

Kobayashi S, Ota Y, Harada Y, et al. (2015) The JRA-55 Reanalysis: General Specifications and Basic Characteristics. J. Met. Soc. Jap., 93(1):5-48, doi:10.2151/jmsj.2015-001.

Livneh B, Bohn T, Pierce D. et al. (2015) A spatially comprehensive, hydrometeorological data set for Mexico, the U.S., and Southern Canada 1950–2013. Sci Data 2, 150042, doi:10.1038/sdata.2015.42.

Marani M, Zanetti S (2015) Long-term oscillations in rainfall extremes in a 268 year daily time series. Water Resources Research 51:639-647, doi:10.1002/2014WR05885.

Martinkova M, Kysely J (2020) Overview of observed Clausius-Clapeyron scaling of extreme preciptiation in mid-latitudes. Atmosphere 11:786, doi:10.3390/atmos11080786.

Maugeri M, Buffoni L, Chlistovsky F (2002) Daily Milan temperature and pressure series (1763-1998): history of the observations and data and metadata recovery. Climatic Change, 53:101-117, doi:10.1023/A:1014970825579

Meehl GA, Tebaldi C, Adams-Smith D (2016) US daily temperature records: past, present and future. Proc. Nat. Amer. Soc. 113:13977-13982, doi:10.1073/pnas.160611711

Moss RH, et al. (2010) The next generation of scenarios for climate change research and assessment. Nature 463:747-756, doi:10.1038/nature08823

Pai D.S, Rajeevan M, Sreejith O.P, Mukhopadhyay B, and Satbha N.S (2014) Development of a New High Spatial Resolution (0.25° × 0.25°) Long Period (1901-2010) Daily Gridded Rainfall Data Set over India and Its Comparison With Existing Data Sets over the Region. MAUSAM 65 (1):1-18, doi:10.54302/mausam.v65i1.851

Powell SB, Delage FPD (2019) Setting and smashing extreme temperature records over the coming decades. Nat Clim Change 9:529-534, doi:10.1038/s41558-019-0498-5

Scolozzi R, Eccel E, (2017) Gli esordi della meteorologia in Trentino nelle fonti d'archivio tra Otto e Novecento. ARCHIVIO TRENTINO, 1: 246-311 (in Italian).

Sillmann J, Kharin VV, Zwiers FW (2013) Climate extremes indices in the CMIP5 multimodel ensemble. Part 2: Future projections. J Geophys Res - Atm 118:2473-2493, doi:10.1002/jgrd.50188

Taylor KE, Stouffer RJ, Meehl GA (2012) An overview of CMIP5 and the experiment design. Bull Am Meteorol Soc, 78:485–498, doi:10.1175/BAMS-D-11-00094.1

Teichmann C, et al. (2021) Assessing mean climate change signals in the global CORDEX-CORE ensemble. Clim Dyn 57:1269-1292, doi: 10.1007/S00382-020-05494-x.

Trenberth KE, Dai A, Rasmussen RM, Parsons DB (2003) The changing character of precipitation. B Am Meteorol Soc 84:1205–1217, doi:10.1175/BAMS-84-9-1205

Trenberth KE, Smith L, Qian T, et al. (2007) Estimates of the global water budegt and its annual cycle using observational and model data. J Hydrometeorol 8:758–769, doi:10.1175/JHM600.1

Vogel, R.M., Zafirakou-Koulouris, A., & Matalas, N.C. (2001) Frequency of record breaking floods in the United States. Water Resoruces Research, 37, 1723 – 1731.

Watanabe M, Suzuki T, O'ishi R, et al. (2010) Improved Climate Simulation by MIROC5: Mean States, Variability, and Climate Sensitivity. Journal of Climate, 23(23):6312-6335, doi:10.1175/2010JCLI3679.1

Yatagai A, Kamiguchi K, Arakawa O, Hamada A, Yasutomi N, and Kitoh A (2012) APHRODITE: Constructing a Long-Term Daily Gridded Precipitation Dataset for Asia Based on a Dense Network of Rain Gauges. B Am Meteorol Soc 93:1401–1415, doi:10.1175/bams-d-11-00122.1, doi:10.1175/BAMS-D-11-00122.1

Tables

Table 1: List of datasets used in the analysis and corresponding regional covers.

Figure Captions

Figure 1. Time series of the frequency of daily precipitation records (see text) found at 4 northern Italian sites: Cavalese, Milano, Padova, Trieste (see Table 1).

Figure 2. Red areas show the observation analysis sub-domains, while boxes show the model analysis domains (land only), which are included in the corresponding CORDEX-CORE simulation domains.

Figure 3. Frequency of occurrence of actual records along with the curve defined by Eq. (1) (left panels) and 10-year running average of the ratio of actual-to-reference frequency of daily precipitation records (RAtR, right panels) based on different gridded station observation datasets and aggregated over seven regions: 3a, from top to bottom, Europe (EUR), North America (NAM), Central America (CAM), Middle East (ME); 3b, from top to bottom, East Asia (EAS),

Southeast Asia (SEA), South Asia (SAS). Also shown in the right panels are the coefficient (units of 1/decade) and p-value of the linear trend fit line of the 10-year running mean values. Underlining indicates cases of statistically significant trends at the 95% confidence level.

Figure 4. 10-year running mean and corresponding linear trend fit line of the RAtR values for the different GCM and RCM CORDEX-CORE simulations over the nine model analysis domains for the period 1970-2099 for the RCP8.5 scenario. The trends are calculated separately for the 1970-2020 historical period and 2020-2099 future period, and for the historical period also corresponding data for the three reanalysis products are reported. The coefficient and p-values of the trend lines (units of 1/decade) are also reported for each dataset (first and second number in parentheses, respectively). Underlining indicates cases of statistically significant trends at the 95% confidence level.

Figure 5. 5a: Linear trend value (units of 1/decade) of the 10-yr running average of the RaAtR value for the historical period 1970-2020 for different reanalysis products, GCM and RCM simulations, over the nine model analysis domains. For the MERRA reanalysis the trend is calculated over the shorter period 1980-2020. Hatching indicates that the trend is statistically significant at the 95% confidence level. 5b: Reanalysis, RCM and GCM multi-model average of the trend values (units of 1/decade) over the period 1970-2020 over the nine model analysis domains.

Figure 6. Coefficients of the linear trend fit line (units of 1/decade) of the 10-year running average RAtR for the period 2020-2099 over the nine model analysis domains and for all RegCM4 and REMO projections in the RCP8.5 scenario. Hatching indicates that the coefficient is statistically significant at the 95% confidence level. Note that for the RegCM4 SAS simulation the driving GCM is not HadGEM but MIROC5 and for the RegCM4 CAM and NAM simulations it is not NorESM but GFDL, which are highlighted with an asterisk in the figure.

Figure 7. Same as Figure 6 but for the RCP2.6 scenario.

Tables

Table 1: List of datasets used in the analysis and corresponding regional covers.

Northern Italy Stations	**Period**	**References**
CAVALESE	1920-2020	Scolozzi et al., 2017
MILANO	1920-2020	Maugeri et al., 2002
PADOVA	1920-2019	Marani et al., 2015
TRIESTE	1924-2020	Cicogna (OSMER)

Observations	**Period**	**Regions**	**References**
APHRO-MA	1951-2007	Monsoon Asia	Yatagai et al., 2012
APHRO-ME	1951-2007	Middle East	Yatagai et al., 2012
E-OBS	1950-2020	Europe	Cornes et al., 2018
IMD	1950-2016	India	Pai et al., 2014
NAmerEXT	1950-2013	North America	Livneh et al., 2015

Reanalyses	**Period**	**Regions**	**References**
ERA5	1950-2020	NAM, CAM, SAM, EUR, SAS, AFR, EAS, SEA, AUS	Hersbach et al., 2020
MERRA-2	1980-2021	NAM, CAM, SAM, EUR, SAS, AFR, EAS, SEA, AUS	Gelaro et al., 2017
JRA-55	1958-2021	NAM, CAM, SAM, EUR, SAS, AFR, EAS, SEA, AUS	Kobayashi et al., 2015

RCMs	**Period**	**Regions**	**References**
RegCM	1970-2099	NAM, CAM, SAM, EUR, SAS, AFR, EAS, SEA, AUS	Giorgi et al., 2012
REMO	1970-2099	NAM, CAM, SAM, EUR, SAS, AFR, EAS, SEA, AUS	Jacob et al., 2012
	driven by the GCMs		**References**
	HadGEM2-ES		Jones et al., 2011
	MPI-ESM-LR		Giorgetta et al., 2013
	MPI-ESM-MR		Giorgetta et al., 2013
	NorESM1-M		Bentsen et al., 2013
	MIROC5		Watanabe et al., 2010
	GFDL-ESM2M		Dunne et al., 2012

Figures

Figure 1:

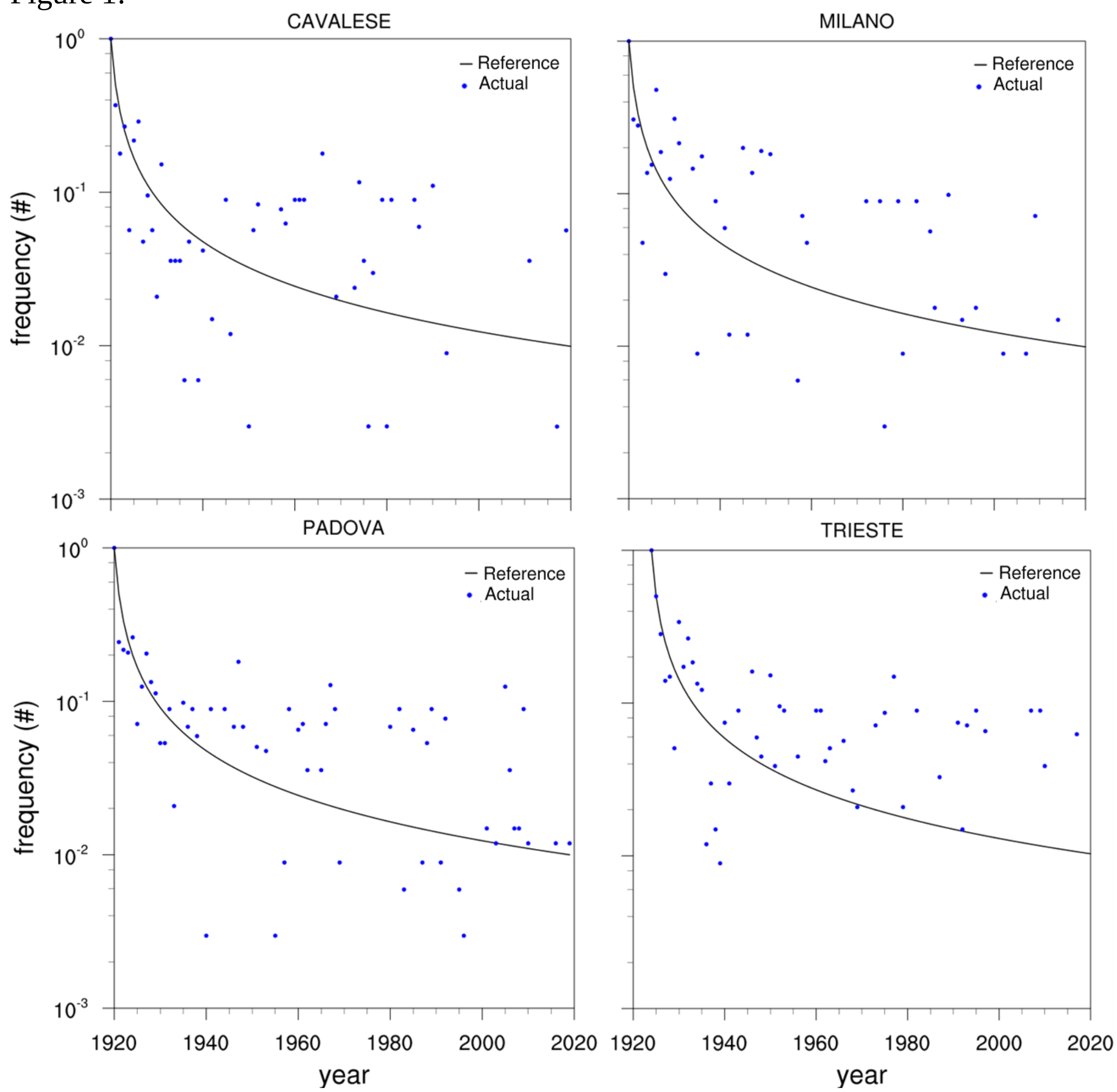

Figure 2:

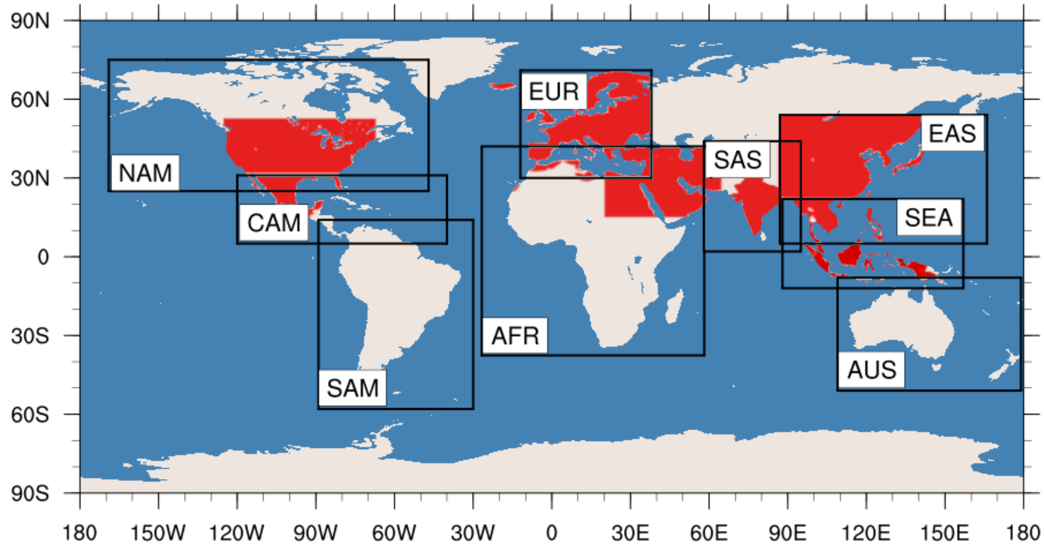

NAM
CAM
SAM
EUR
AFR
SAS
EAS
SEA
AUS
90N
60N
30N
0
30S
60S
90S
180
150W
120W
90W
60W
30W
0
30E
60E
90E
120E
150E
180

Figure 3a:

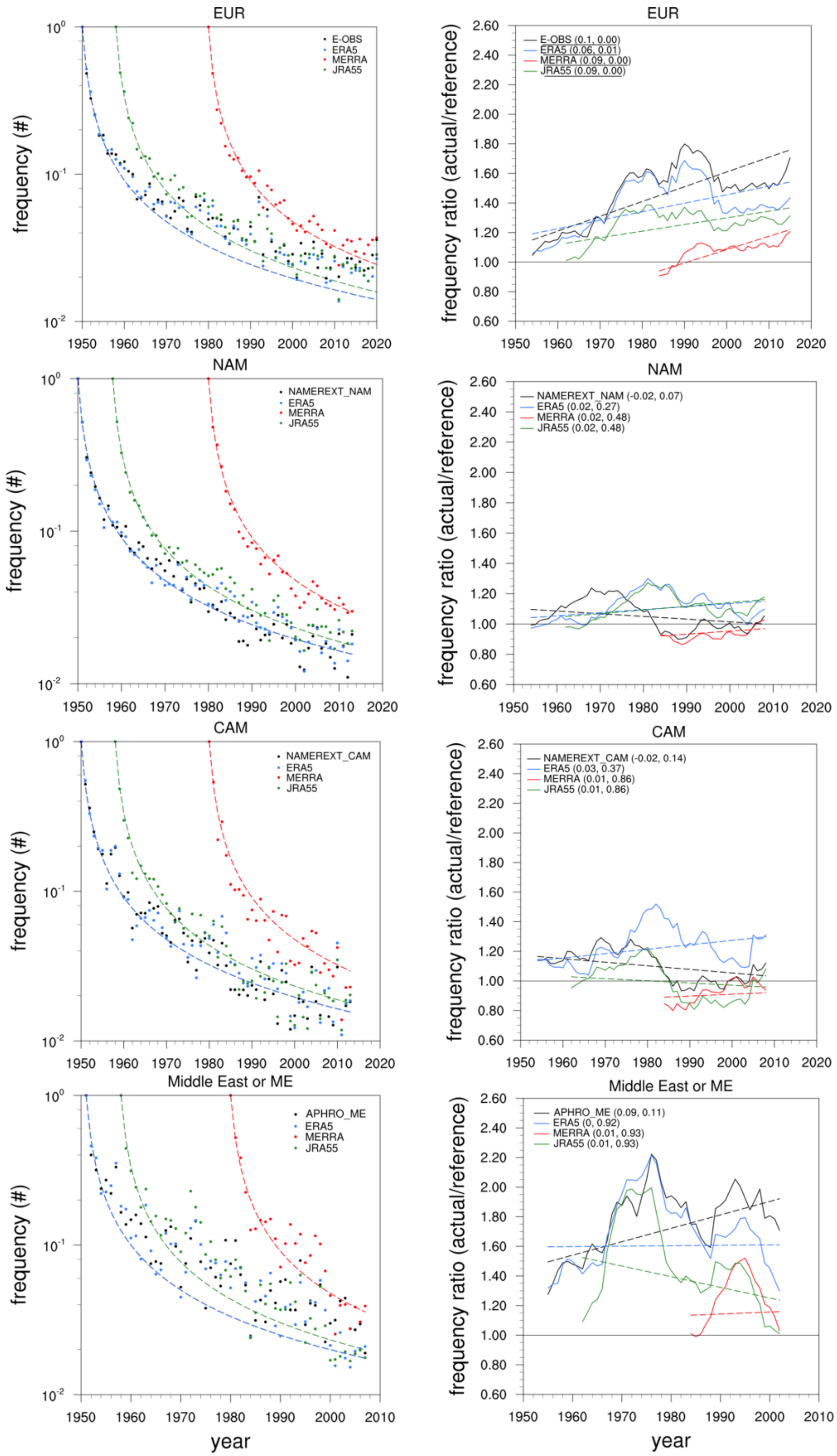
EUR
E-OBS
ERA5
MERRA
JRA55
frequency (#)
EUR
E-OBS (0.1, 0.00)
ERA5 (0.06, 0.01)
MERRA (0.09, 0.00)
JRA55 (0.09, 0.00)
frequency ratio (actual/reference)
NAM
NAMEREXT_NAM
ERA5
MERRA
JRA55
frequency (#)
NAM
NAMEREXT_NAM (-0.02, 0.07)
ERA5 (0.02, 0.27)
MERRA (0.02, 0.48)
JRA55 (0.02, 0.48)
frequency ratio (actual/reference)
CAM
NAMEREXT_CAM
ERA5
MERRA
JRA55
frequency (#)
CAM
NAMEREXT_CAM (-0.02, 0.14)
ERA5 (0.03, 0.37)
MERRA (0.01, 0.86)
JRA55 (0.01, 0.86)
frequency ratio (actual/reference)
Middle East or ME
APHRO_ME
ERA5
MERRA
JRA55
frequency (#)
year
Middle East or ME
APHRO_ME (0.09, 0.11)
ERA5 (0, 0.92)
MERRA (0.01, 0.93)
JRA55 (0.01, 0.93)
frequency ratio (actual/reference)
year

Figure 3b:

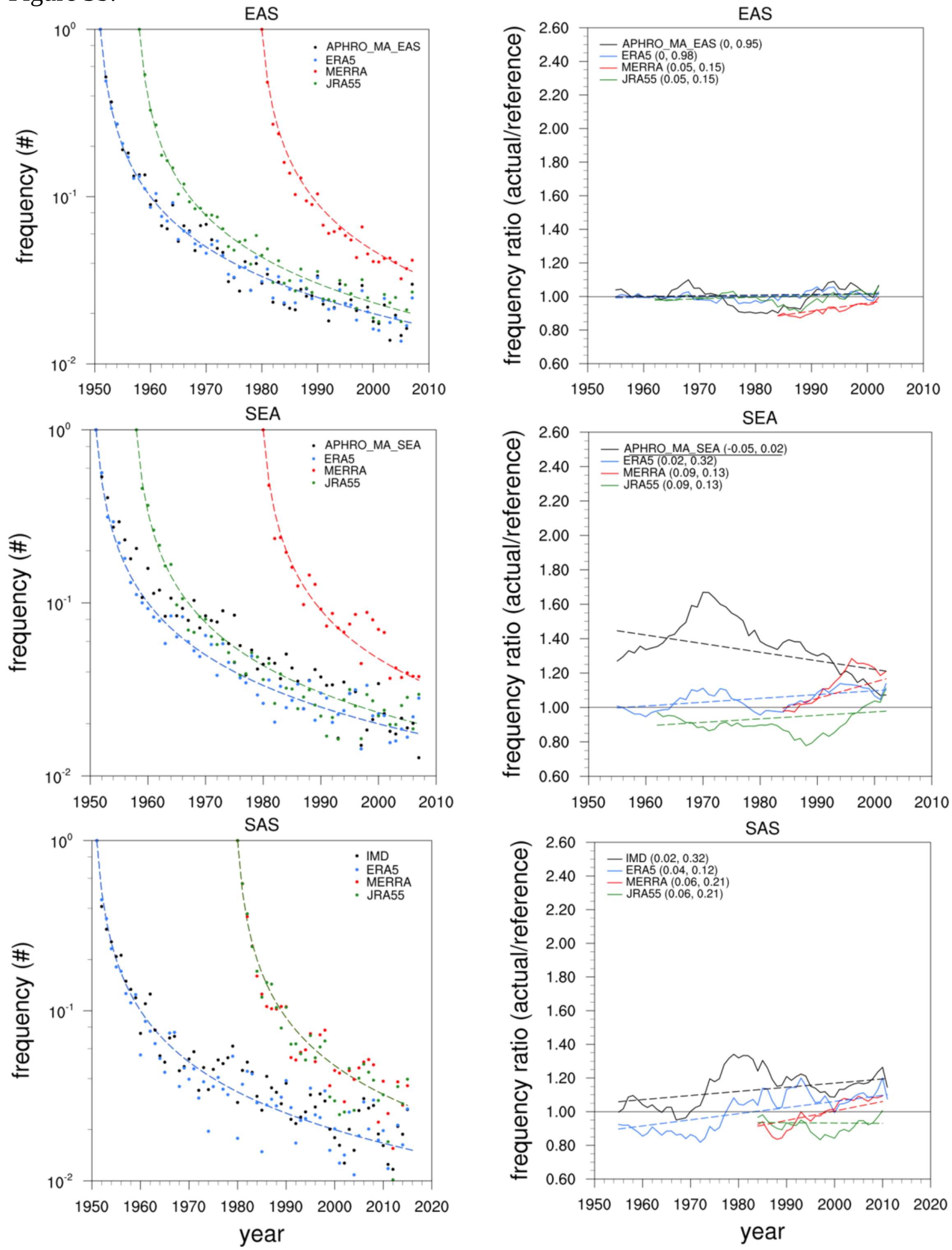
EAS
APHRO_MA_EAS
ERA5
MERRA
JRA55
frequency (#)
EAS
APHRO_MA_EAS (0, 0.95)
ERA5 (0, 0.98)
MERRA (0.05, 0.15)
JRA55 (0.05, 0.15)
frequency ratio (actual/reference)
SEA
APHRO_MA_SEA
ERA5
MERRA
JRA55
frequency (#)
SEA
APHRO_MA_SEA (-0.05, 0.02)
ERA5 (0.02, 0.32)
MERRA (0.09, 0.13)
JRA55 (0.09, 0.13)
frequency ratio (actual/reference)
SAS
IMD
ERA5
MERRA
JRA55
frequency (#)
year
SAS
IMD (0.02, 0.32)
ERA5 (0.04, 0.12)
MERRA (0.06, 0.21)
JRA55 (0.06, 0.21)
frequency ratio (actual/reference)
year

Figure 4:

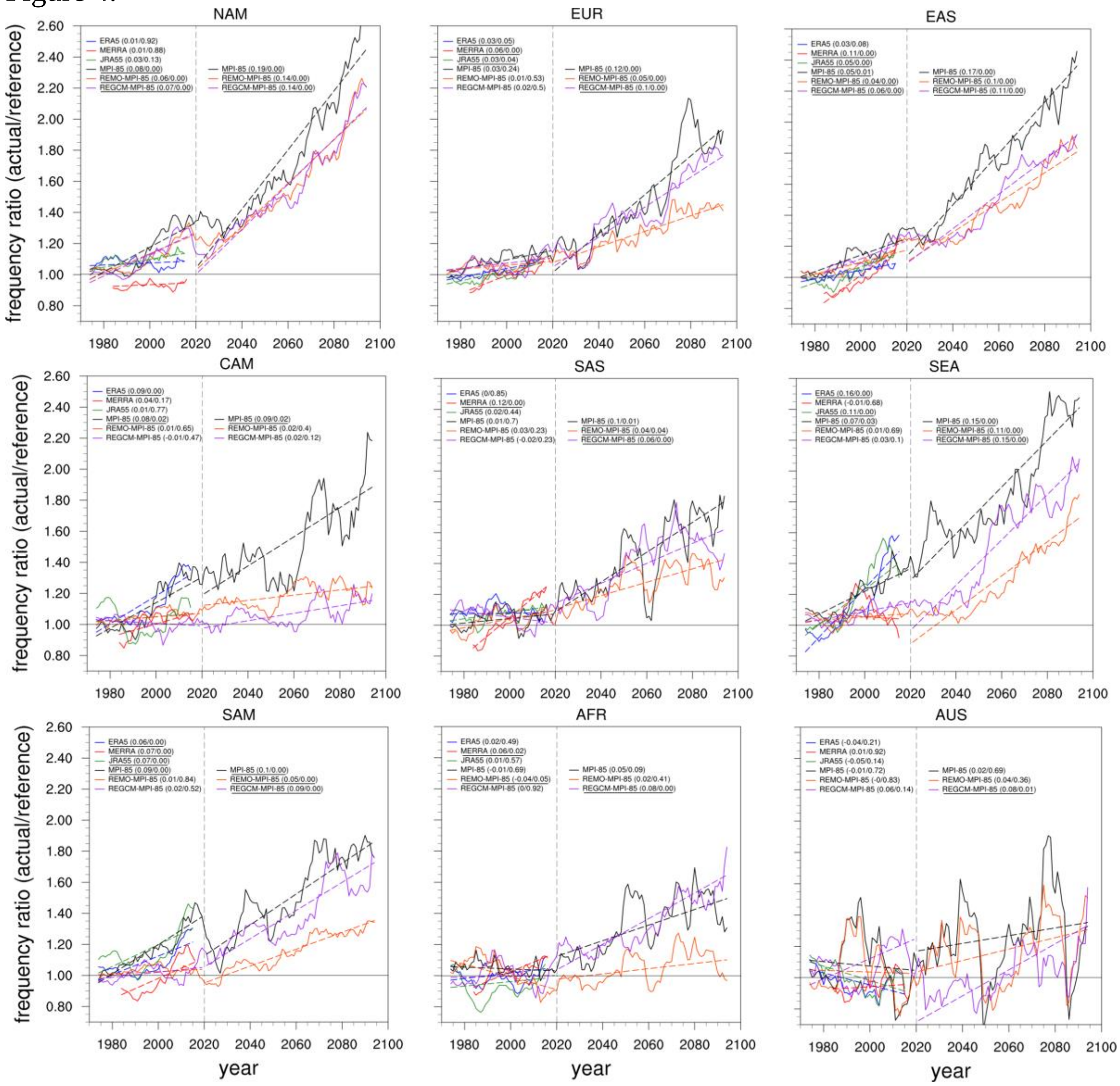

NAM
EUR
EAS
CAM
SAS
SEA
SAM
AFR
AUS
frequency ratio (actual/reference)
year

Figure 5a:

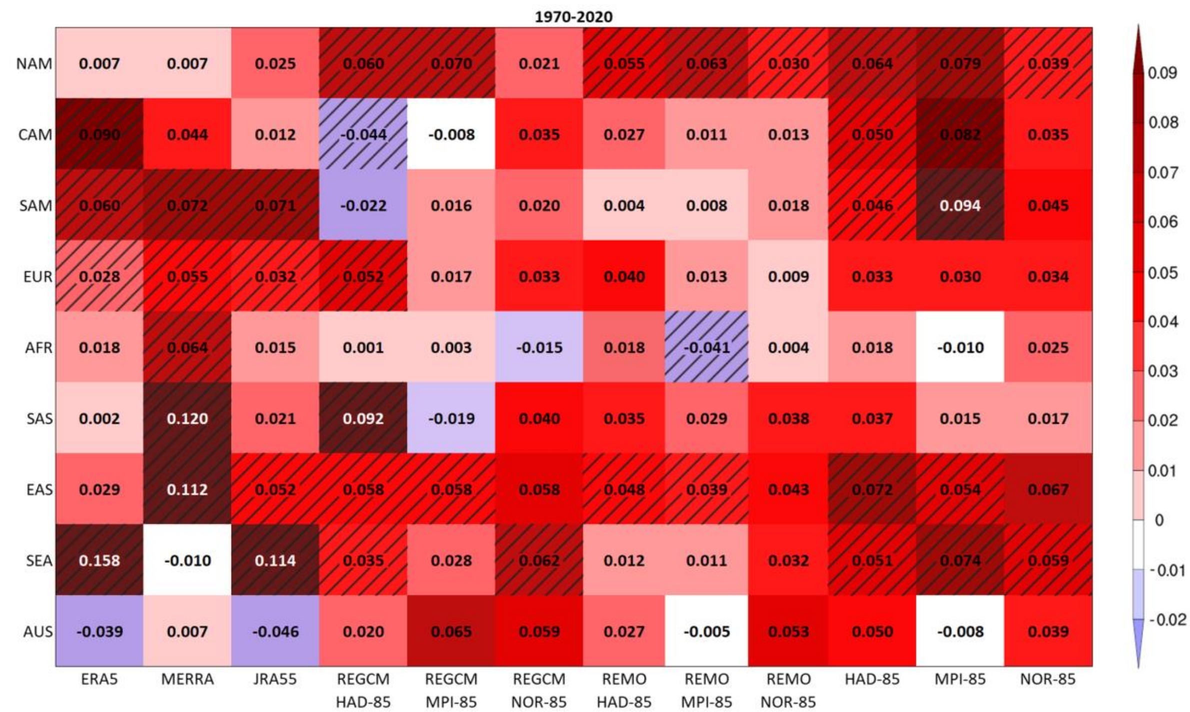

Figure 5b:

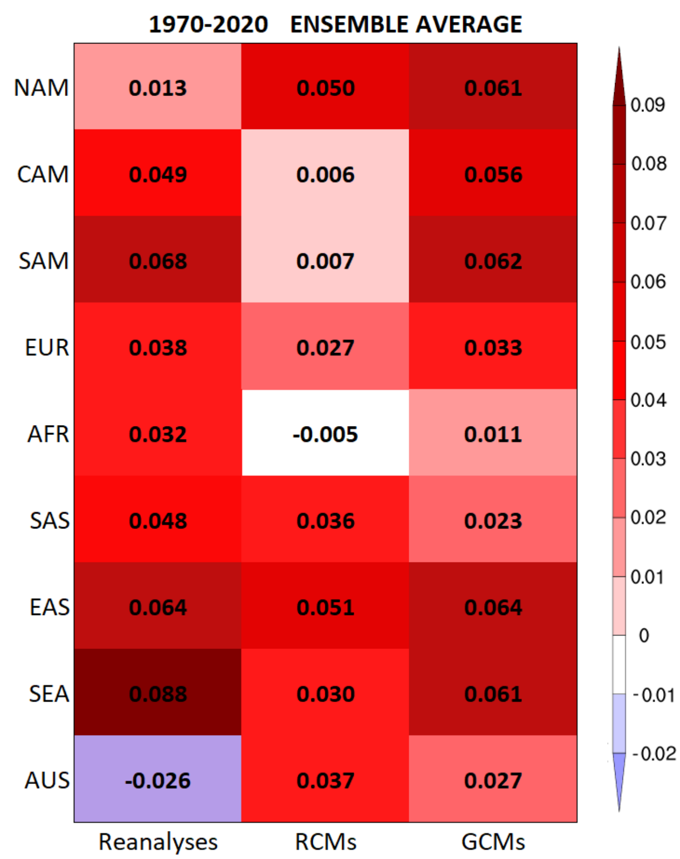

Figure 6:

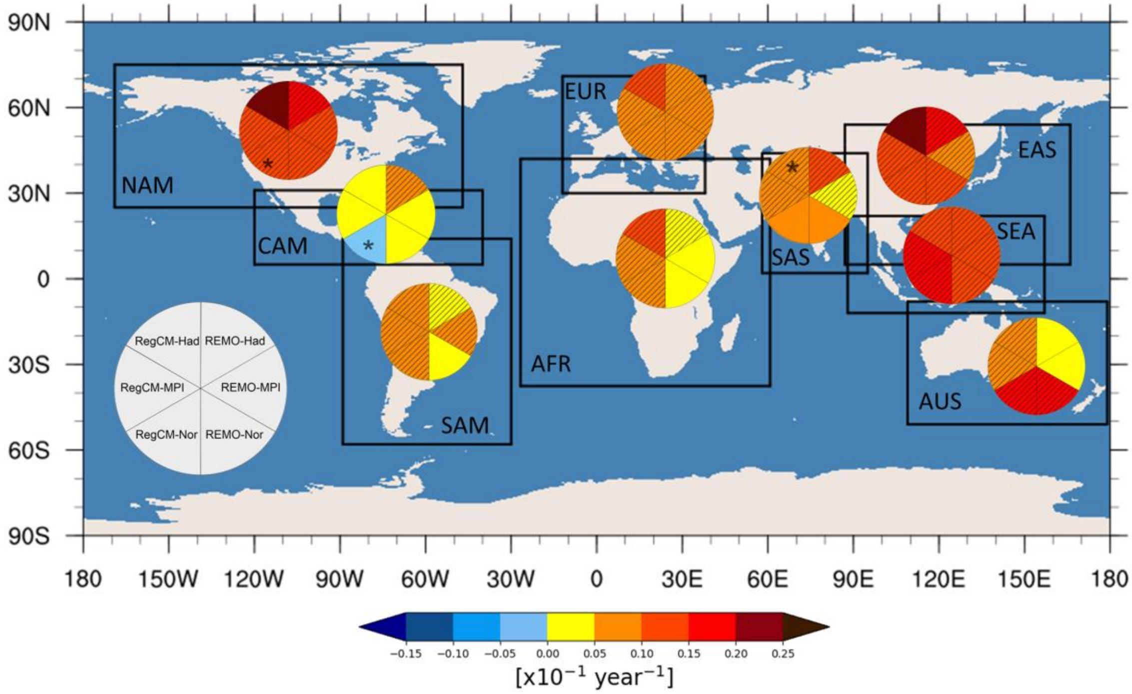

Figure 7: